European Science Review 2025,
No 7-8
ISSN 2310-5577

PREMIER Publishing
ppublishing.org

Section 1. Chemistry

DOI:10.29013/ESR-25-7.8-3-14

STUDY ON THE PHOSPHORUS REMOVAL MECHANISM AND APPLICATION POTENTIAL OF FE/N-MODIFIED BIOCHAR

Yiming Gao [1]

[1] Lower Merion High School, United States

Cite: *Yiming Gao (2025). Study on the Phosphorus Removal Mechanism and Application Potential of Fe/N-modified biochar. European Science Review 2025, No 7–8.* https://doi.org/10.29013/ESR-25-7.8-3-14

Abstract

Phosphorus is a key nutrient limiting the primary productivity of lakes, but its excessive input has become the main cause of eutrophication. To address both phosphorus pollution in water bodies and the need for resource recovery, this paper developed an iron-nitrogen co-modified biochar (Fe/N-BC) using agricultural wastes as the raw material. The modified biochar was produced through the co-pyrolysis of $FeCl_3$ and urea and achieved improvements in both structure and function. Its structure was characterized using BET and FTIR techniques. Its phosphate removal performance and adsorption behavior were investigated through batch adsorption experiments and were analyzed by kinetic and isothermal models, respectively. The results showed that Fe/N-BC possessed a high specific surface area (916.5 m^2/g) and a well-developed microporous structure, with a maximum phosphorus adsorption capacity of 31.34 mg/g, which outperformed that of raw biochar and attapulgite (a control material). The adsorption process conforms to a pseudo-second-order kinetic model, indicating chemisorption as the dominant mechanism. FTIR analysis revealed the formation of Fe–O–P bonds and hydrogen bonding interactions involving pyrrolic-N, showing a synergistic adsorption system. At pH 5 and with coexisting Cl/SO_4^{2-} ions, Fe/N-BC still showed good adaptability and resistance to interference. Furthermore, in actual lake water, the material maintained stable phosphorus removal performance, proving its strong environmental adaptability and potential for engineering applications. The Fe/N co-modification in this study strategy helps deepen the understanding of phosphorus adsorption and build a practical foundation for creating more effective materials to control eutrophication in water bodies.

Keywords: *Phosphorus removal; Biochar; Fe/N co-modification; Adsorption mechanism; Eutrophication control*

1. Introduction

Phosphorus (P) is a key limiting nutrient for primary productivity in lake ecosystems and plays a vital role in the growth and metabolism of aquatic organisms. However, when excessive amounts of phosphorus enter the

water, it can lead to eutrophication (Qian et al., 2023). The sources of excessive P include point sources such as industrial discharges and municipal wastewater, and non-point sources like agricultural runoff (Luo et al., 2023). According to the United Nations Environment Programme (UNEP), eutrophication can lead to dissolved oxygen depletion, loss of biodiversity, and threats to drinking water safety. Therefore, it is important to develop effective and sustainable phosphorus removal and recovery strategies.

There are different techniques for phosphorus removal from water bodies. Biological methods involve polyphosphorus bacteria taking up phosphorus aerobically and releasing it anaerobically, and through sludge discharge, phosphorus absorbed by microorganisms is removed from the system (Pan et al., 2024). However, this process requires precisely controlled environmental conditions (Zubrowska-Sudol & Walczak, 2015). Physicochemical methods mainly include chemical processes and adsorption. Chemical processes can remove phosphorus effectively, but they also require large quantities of reagents, have high sludge production, and potentially produce secondary pollution (Pan et al., 2024). In contrast, adsorption is considered a promising technique for its low cost, high removal efficiency, easy operation, absence of secondary pollution (Mei et al., 2021), and wide applications across different treatment conditions (Cheng et al., 2023).

Biochar is produced from biomass through pyrolysis. It is a suitable adsorbent for phosphorus because it has a high specific surface area, well-developed porosity, and rich functional groups (Lin et al., 2024), and can support carbon neutrality goals (Li et al., 2022). Among biochar modification techniques, Fe modification provides functional groups and generates pore structures, making it one of the most widely used methods (Yi et al., 2021). Still, Fe modification alone produces an insufficient number of functional groups (Li & Shi, 2022). According to Liu et al. 2020, the N-doping method added more nitrogen-containing functional groups like pyridinic N and pyrrolic N. The electron pairs of nitrogen functional groups can also facilitate electron exchange in adsorption processes (Zhou et al., 2018) and thus improve electron transfer. Consequently, this study presents an iron and nitrogen co-modified biochar (Fe/N-BC) with rice straw as the raw material. This biochar was produced through one-step pyrolysis of rice straw pre-treated with $FeCl_3$ and urea to improve the phosphate adsorption efficiency. Fe–N co-modification improved biochar's properties by increasing surface area, creating more pore structure and functional groups, introducing magnetic components, and improving hydrophilicity and polarity (Mei et al., 2021). Moreover, rice straw biochar can help mitigate the issue of over 100 million tonnes burned directly and reduce greenhouse gas emissions, and serve as a soil amendment and a slow-release fertilizer because of its high porosity, large surface area, and high cation exchange capacity (CEC) (Singh et al., 2025).

Currently, few studies have examined Fe-N-modified biochar as an adsorbent or investigated how this co-modification alters its physicochemical properties (Mei et al., 2021). This study analyzed Fe/N-BC's phosphate adsorption behavior and structure characteristics through kinetics and isothermal models, and FTIR analysis of Fe/N synergistic mechanisms. Also, this study investigated the effects of varying pH, coexisting ions (like Cl^-, $SO4^{2-}$), and ion strength on adsorption behavior; Eventually, phosphorus removal experiments were conducted using actual water samples to evaluate the material's environmental adaptability and application prospects. Moreover, this study selected attapulgite, a natural clay mineral, as a comparison material to assess Fe/N-BC's adsorption performance. The study results proved that Fe–N co-modification is an effective method to improve the biochar's adsorption performance on phosphorus. This study aims to provide a scientific foundation for developing effective phosphate adsorbents to control lake eutrophication and achieve sustainable phosphorus resource management.

2. Materials and methods

2.1 Preparation of adsorption materials

Three adsorption materials were used in this study, including raw rice straw biochar, iron-nitrogen modified rice straw biochar, and attapulgite clay.

Raw Rice Straw Biochar (RSBC**):** 10 g of rice straw mixed with deionized water and

stirred on a magnetic stirrer for 24 hours. After centrifugation, the solid was dried in an oven at 80 °C. The dried samples were then placed in a quartz boat and pyrolyzed in a tube muffle furnace (OTF-1200X-S). The heating rate was set to 5 °C/min, and the temperature was held at 700 °C for 2 hours before cooling to room temperature. The resulting solid was washed with deionized water until nearly neutral, dried again, and ground using a ball mill. The final product was sieved through a 100-mesh screen to obtain uniform raw rice straw biochar.

Iron/Nitrogen Co-Modified Rice Straw Biochar: 10 g of rice straw, 50 g of $FeCl_3 \cdot 6H_2O$, and 12 g of urea were dissolved in 200 mL of deionized water. The mixture was stirred on a magnetic stirrer for 24 hours, then centrifuged and dried in an oven at 80 °C. The dried solid was subsequently pyrolyzed, washed, ground, and passed through a 100-mesh sieve to obtain uniform Fe/N-modified rice straw biochar.

Attapulgite: The attapulgite used in this study was sourced from Mingguang City, Anhui Province, China. It was obtained by grinding natural attapulgite clay and sieving it through a 100-mesh screen.

2.2 Phosphate Adsorption Kinetics

Accurately weigh approximately 0.20 g of the adsorbent material into a centrifuge tube and add 500 mL of phosphate solution at a concentration of 30 mg/L. Place the mixture at 25 °C and perform constant-temperature shaking. Sample for 0, 5, 10, 20, 30 minutes and 1, 2, 3, 4, 6, 8, 10, 12, and 24 hours, then filter the solution through a 0.45 μm membrane to determine the phosphate concentration in the filtrate.

The phosphorus adsorption kinetics processes of different materials were fitted using pseudo-first-order and pseudo-second-order adsorption kinetics models, and the calculation formulas were Formula (1) and Formula (2), respectively:

$$\ln\left(q_e - q_t\right) = \ln q_e - k_1 t \quad (1)$$

$$\frac{t}{q_t} = \frac{1}{k_2 q_e^2} + \frac{t}{q_e} \quad (2)$$

where q_t represents the amount of phosphate adsorbed by each material at time t (mg/g), q_e is the adsorption capacity of each material at equilibrium (mg/g), k_1 is the adsorption rate constant in the pseudo-first-order kinetic model, and k_2 is the adsorption rate constant in the pseudo-second-order kinetic model.

2.3 Phosphate Adsorption Isotherms

Weigh 0.030 g of the adsorbent material into a centrifuge tube and separately add 200 mL of phosphate solutions (KH_2PO_4) with concentrations of 10, 30, 50, 100, 150, 200, 500, and 1000 mg/L. Shake the mixture at 25 °C for 24 hours at a constant temperature, then filter through a 0.45 μm membrane. The phosphate concentration in the filtrates is then measured.

The phosphate adsorption isotherms of five materials were fitted using Freundlich and Langmuir isotherm models. The corresponding equations are:

$$q_e = K_F C_e^{1/n} \quad (3)$$

$$\frac{C_e}{q_e} = \frac{1}{q_{max} K_L} + \frac{C_e}{q_{max}} \quad (4)$$

where *qe* is the amount of phosphate adsorbed by each material at equilibrium (mg/g), q_{max} represents the maximum adsorption capacity of each material (mg/g), *KL* is the Langmuir constant, *KF* is the Freundlich constant, n indicates the adsorption intensity, and *Ce* is the equilibrium concentration of phosphate in the solution.

2.4 Influencing Factors

2.4.1 Influence of pH

To investigate the effect of pH value on the phosphorus adsorption efficiency of different materials, HCl and NaOH were used to adjust the initial pH values of the solution to 5, 6, 7, 8, 9, and 10, respectively, with an ion strength of 0.1 mM. The remaining steps follow those described in Section 2.3.

2.4.2 Type of Coexisting Ions

Add 0.030 g of dried adsorbent material to a centrifuge tube and set the initial phosphate concentration to 40 mg/L. Choose F^-, Cl^-, SO_4^{2-}, CO_3^{2-}, K^+ and Ca^{2+} as co-existing ions, each at a concentration of 0.1 mm. The remaining steps follow those described in Section 2.3.

2.4.3 Ionic Strength

Weigh approximately 0.030 g of each adsorbent material into centrifuge tubes and

control the initial phosphate concentration at 40 mg/L. Adjust the ionic strength for each set in a range of 0 to 0.2 mM. The remaining steps follow those described in Section 2.3.

2.5 Application to Phosphate Removal in Actual Water Bodies

To further verify the phosphate removal performance of raw biochar, attapulgite, and Fe/N-modified biochar in real water bodies, representative samples were collected from urban rivers and lakes. Phosphate concentrations in the water samples were measured before and after adsorption. After filtration through a 0.45 μm membrane to remove suspended particulate matter, 100 mL of each river or lake sample was mixed with 15 mg of the corresponding adsorbent. The mixtures were shaken at room temperature for 4 h and then filtered again through a 0.45 μm membrane. Phosphate removal efficiency was calculated based on concentration differences before and after adsorption.

3. Results and Discussion

3.1 Material Characteristics and Pore Structure

The specific surface area of the iron/nitrogen co-modified biochar (Fe/N-BC) reached 916.5 m²/g, which is 6.8 times greater than that of unmodified biochar (133.8 m²/g) (Table 1). These results indicate that the co-pyrolysis of $FeCl_3$ and urea significantly enhanced pore development. During pyrolysis at 700 °C, the molten salt effect of $FeCl_3$ and NH_3 released from urea decomposition worked together to accelerate the gasification reaction of the carbon matrix and formed a microporous-mesoporous hierarchical structure (microporous volume of 0.66 cm³/g, total pore volume of 0.94 cm³/g). This result is consistent with the synergistic pore-making effect of HNO_3 oxidation and Fe^{2+} loading (Li et al., 2020). In contrast, the attapulgite material (147.5 m²/g) showed weak pore development due to the limitation of the silicate mineral crystal structure, with a relatively low total pore volume 0.085 cm³/g. Clearly, the iron-nitrogen co-modification strategy effectively overcomes the agglomeration effect of conventional iron-based biochar, and its specific surface area far exceeds that of Fe-BC (10––12.5 m²/g) (Li B. et al., 2021).

Table 1. *Comparison of Specific Surface Area and Pore Characteristics of Different Materials*

Index	Pristine biochar	Iron-nitrogen-modified biochar	Attapulgite
Specific surface area ($m^2 \cdot g^{-1}$)	133.8	916.5	147.5
Total pore volume ($cm^3 \cdot g^{-1}$)	0.086	0.94	0.085
Micropore volume ($cm^3 \cdot g^{-1}$)	0.052	0.66	0.058
Micropore porosity (%)	60.4	70.2	68.2

3.2 Phosphate Adsorption Kinetics

The iron/nitrogen co-modified biochar reached the adsorption equilibrium within 24 h, with an equilibrium adsorption capacity of 18.75 mg/g (q_e = 18.75 mg/g). The adsorption was 4.7 and 3.7 times higher than that of unmodified biochar (3.98 mg/g) and attapulgite (5.07 mg/g), respectively (Table 2). The adsorption process was more in line with the pseudo-second-order kinetic model (R^2 = 0.99). Therefore, the dominant mechanism was chemisorption, which includes ligand exchange between Fe^{3+} and PO_4^{3-} and electrostatic attraction of nitrogen functional groups (Li & Shi, 2022). It is noteworthy that the apparent rate constant of the Fe-N material (k_2 = 0.24 g/(mg-min)) was lower than that of the attapulgite (0.61 g/(mg-min)), which may be related to the mass transfer resistance of the microporous structure, but its adsorption amount at equilibrium (18.75 mg/g) is still significantly higher than that of attapulgite (Figure 1).

Figure 1. *Kinetics of phosphorus adsorption by different materials*

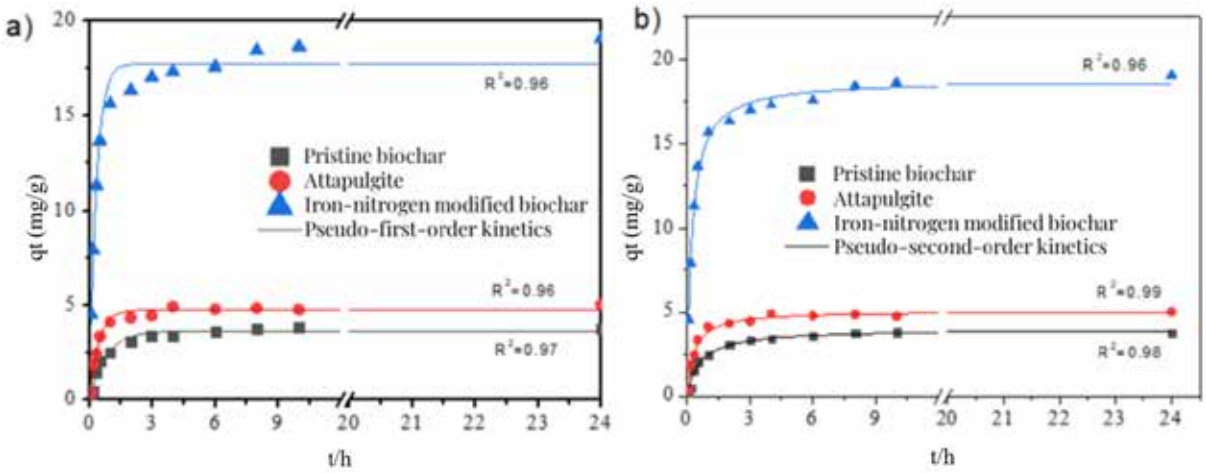

(a) Pseudo-first-order kinetic model fitting (b) Pseudo-second-order kinetic model fitting

Table 2. *Adsorption kinetics Parameters of Biochar and Its modified materials*

Materials	Proposed-first-order kinetics			Pseudo-second-order kinetics		
	q_e (mg/g)	k_1 (1/min)	R^2	q_e (mg/g)	k_2 (g/mg*min)	R^2
Pristine biochar	3.63	1.25	0.97	3.98	0.40	0.98
Attapulgite	4.74	2.26	0.96	5.07	0.61	0.96
Iron-nitrogen-modified biochar	17.74	3.09	0.96	18.75	0.24	0.99

3.3 Phosphate Adsorption Isotherms and Capacity

Figure 2. *Isotherms of phosphorus adsorption for different materials*

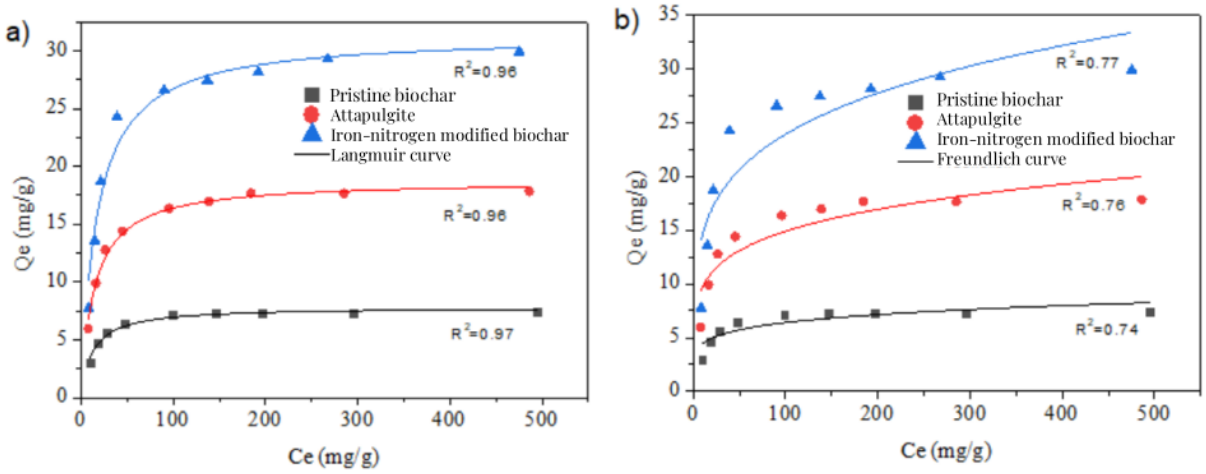

(a) Langmuir isotherm fitting for pristine biochar, attapulgite, and iron–nitrogen modified biochar

(b) Freundlich isotherm fitting for pristine biochar, attapulgite, and iron–nitrogen modified biochar

Langmuir model fitting showed (Table 3) that the maximum adsorption capacity of Fe/N-BC (q_m = 31.34 mg/g) was 3.98 times higher than that of unmodified biochar (7.87 mg/g). These results suggested that Fe–N co-modification greatly enhanced raw biochar's phosphorus adsorption capacity. Reported values for other materials, such as Mg/Al-modified biochar (6.10 mg/g) (Li S. et al., 2021) and Fe-BC690 (26.14 mg/g) (Li B. et al., 2021), suggest that Fe/N-BC had a comparatively high adsorption capacity. The Freundlich constant (K_F = = 8.94 L/mg) indicated a high density of heterogeneous adsorption sites on the surface of the material, and the $^1/_n$ value (0.21) showed moderate adsorption intensity, suggesting a moderate affinity for phosphate (Figure 2). While its isotherm performance is still below that of Mg-modified coffee grounds biochar (q_m = 63.5 mg/g) (Shin et al., 2020), Fe/N-BC offers greater advantages in terms of raw material costs and regeneration potential.

Table 3. *Isotherm parameters of phosphorus adsorption for different materials*

Materials	Langmuir adsorption model			Freundlich adsorption model		
	q_m(mg/g)	K_L(L/mg)	R^2	K_F(L/mg)	1/n	R^2
Pristine biochar	7.87	0.08	0.97	3.07	0.16	0.74
Iron-nitrogen-modified biochar	31.34	0.05	0.96	8.94	0.21	0.77
Attapulgite	18.75	0.05	0.96	6.34	0. 19	0.76

3.4 Influence of environmental factors

The varying pH of the solution affects the adsorption capacity and surface properties of biochar and chemical forms of phosphate in solution (Hou et al., 2020). In addition, phosphorus adsorption is affected by coexisting anions in the solution (Luo et al., 2023), which compete with the phosphate ions for adsorption sites. The presence of anions such as Cl^-, F^-, SO_4^{2-}, and HCO_3^- can inhibit phosphate uptake. As shown in Figure 4a, Fe/N-BC consistently showed the highest phosphate adsorption capacity across all pH values (5–10). When pH < 7, phosphate primarily exists as $H_2PO_4^-$, which was easily complexed with metal sites on the surface of the material (e.g., Fe^{3+}) (Ping et al., 2023), and thus Fe/N-BC had a higher adsorption capacity at lower pH. The best adsorption performance of Fe/N-BC (25.1 mg/g) was obtained at pH = 5, which was consistent with the optimal adsorption pH of γ-Al_2O_3/Fe_3O_4-modified biochar (Cui et al., 2020).

Moreover, the change in pH has different effects on phosphorus adsorption. According to Luo et al. 2023, at pH below the point of zero charge (pHpzc) of the biochar, surface functional groups become protonated and positively charged, thus enhancing the adsorption of anionic phosphate species through electrostatic attraction. As the solution pH increases, surface groups become deprotonated and negatively charged, leading to a reduced adsorption capacity (Luo et al., 2023).

Under the influence of coexisting ions and different ion strengths, the results showed that the adsorption capacity of pristine biochar, iron-nitrogen-modified biochar, and attapulgite on phosphorus all exhibited slight fluctuations (Figure 3). These slight changes indicate that the influence of environmental ions on phosphorus adsorption of the three materials is relatively small. The findings are consistent with the chemisorption mechanism supported by kinetic and spectroscopic analyses. In addition, it can be seen that under the ion type and ion strength conditions, the adsorption capacity of iron-nitrogen-modified biochar for phosphorus was consistently higher than that of pristine biochar and attapulgite, further demonstrating its enhanced adsorption capacity.

Figure 3. *Effect of pH, coexisting ion types, and ion concentrations on phosphate adsorption capacity*

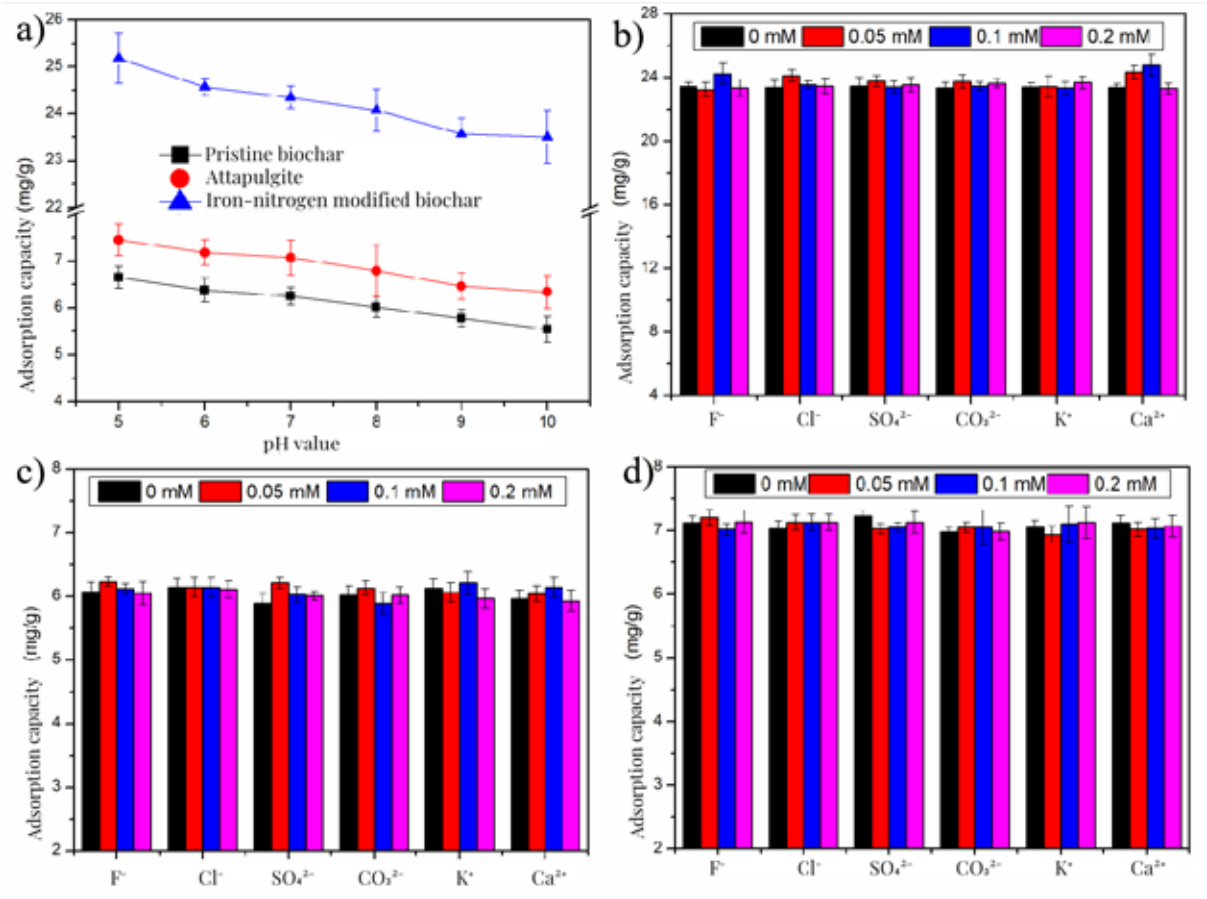

(a) Influence of pH value on the adsorption capacity of pristine biochar, attapulgite, and iron-nitrogen-modified biochar.

(b) Influence of different coexisting ions and their concentrations on adsorption by iron-nitrogen-modified biochar.

(c) Influence of different coexisting ions and their concentrations on adsorption by pristine biochar.

(d) Influence of different coexisting ions and their concentrations on adsorption by attapulgite.

3.5 Adsorption Mechanism Analysis

Generally, the adsorption mechanisms of the phosphate adsorption adsorbent are electrostatic interaction, ion exchange, surface complexation, and precipitation (Huang et al., 2024). In this study, Fe/N-BC's enhanced capacity is mainly due to its surface chemical structure and the synergistic effect of multiple adsorption mechanisms. Firstly, iron modification provided essential phosphate-binding sites. After phosphate was adsorbed onto Fe/N-BC, a distinct Fe–O–P vibration band appeared in the FTIR spectrum at approximately 1120 cm^{-1} (Figure 4). This feature indicates that phosphate ions formed stable complexes or precipitates with Fe^{3+}/FeOOH through ligand exchange or surface complexation. Secondly, nitrogen doping introduced electron-rich functional groups such as pyrrolic-N, amino (–NH_2), and amide groups. This modification greatly increased the surface electron density and hydrophilicity of the material. Also, the decreased intensity of the pyrrole-N peak at 1620 cm^{-1} (Figure 4) suggests that nitrogen functional groups are involved in adsorption through hydrogen bonding. Together, these properties made the material more favorable for interacting with phosphate ions.

In addition to the chemical transformations mentioned above, Fe and N also work together during material formation to shape the structure of the material. Firstly, $FeCl_3$

acted as the pore-forming component during pyrolysis. It promoted the formation of hierarchical micro-, meso-, and macro-pores. These pores facilitated the transport of phosphates and served as additional routes for phosphate dispersion (Yang et al., 2011). Also, the decomposition of urea released gases such as ammonia (NH_3) and carbon dioxide (CO_2) (Xiang et al., 2012). These gases expanded the carbon framework, especially contributing to the formation of mesopores that further increased the specific surface area and the amount of surface active sites. Together, both Fe and N provided the material with the advantages of both high porosity and a high content of surface functional groups.

Moreover, electrostatic attraction and surface precipitation also contribute to phosphate removal (Wu et al., 2020). Under low pH conditions, the material surface is positively charged, which favors the adsorption of negatively charged species such as $H_2PO_4^-$ and HPO_4^{2-}. In neutral to alkaline environments, Fe^{3+} can further react with PO_4^{3-} to form precipitates like $FePO_4$ to reduce phosphate concentrations in solution (Li et al., 2018).

Figure 4. *Comparison of FTIR spectra of the three materials before and after phosphorus adsorption*

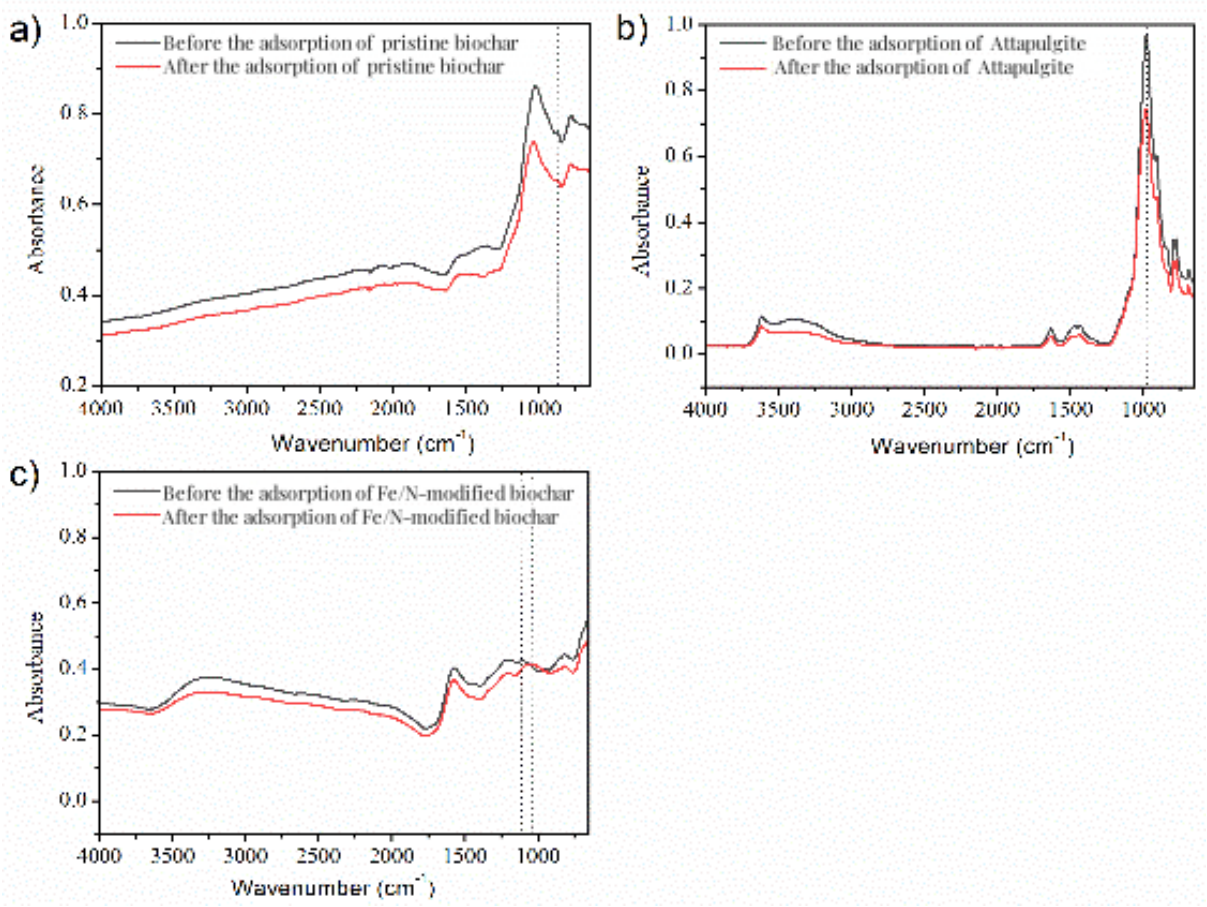

(a) Pristine biochar before and after adsorption;

(b) Attapulgite before and after adsorption;

(c) Fe/N–modified biochar before and after adsorption.

3.6 Practical Application Potential

One important indicator of a phosphorus adsorbent's effectiveness in real-world applications is how well it removes phosphorus from actual water sources. In this study, Fe/N-BC maintained good phosphorus removal performance in real river and lake wa-

ter samples, with a removal rate of 75% and nearly 80% respectively (Figure 5). This result reflects its strong adsorption capacity and environmental adaptability. Its strong resistance to interference is likely due to the selective binding of the surface Fe–O active sites and nitrogen-containing functional groups toward phosphate ions. Therefore, compared to pristine biochar and attapulgite, Fe/N-BC had a more stable performance and was less affected by environmental conditions, which include coexisting organic matter, anions, and slight pH fluctuations. Moreover, because of its advantages, such as strong environmental compatibility and cost-effectiveness, Fe/N-BC shows great promise for application in real-world scenarios. Potential applications include agricultural runoff treatment, eutrophication control in lakes, and phosphorus recovery from wastewater for sustainable reuse.

Figure 5. *Comparison of the phosphorus adsorption effects of three adsorption materials on actual water bodies*

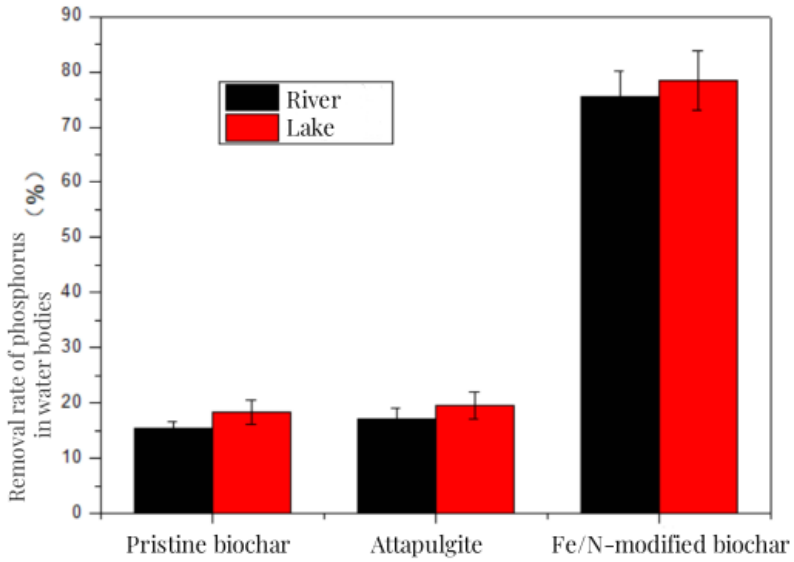

4. Conclusion

This study introduced an iron/nitrogen co-modified biochar (Fe/N-BC), produced by pretreating rice straw with $FeCl_3$ and urea and followed by one-step pyrolysis, and evaluated its potential for phosphorus removal. Results showed that Fe/N-BC had a highly porous structure with a specific surface area of 916.5 m^2/g, exceeding that of raw biochar and attapulgite. Regarding adsorption kinetics and capacity, the adsorption process followed the pseudo-second-order kinetics model and indicated chemisorption as the dominant mechanism; Fe/N-BC achieved a maximum phosphate adsorption capacity of 31.34 mg/g, the highest among all tested materials. FTIR analysis showed that both Fe–O–P complexation and nitrogen-containing functional groups toward phosphate ions contributed to effective phosphate removal. Under the influence of varying pH, coexisting ions, and different ion strengths, Fe/N-BC still maintained the highest adsorption capacity among the tested materials. Most importantly, in real river and lake samples, Fe/N-BC had a stable phosphorus removal performance with nearly a 75% and nearly an 80% removal rate, respectively, and showed its potential for mitigating eutrophication. By analyzing its structural characteristics, adsorption kinetics and capacity, influencing factors, and application in real-world water samples, this study proved the Fe–N co-modification technique to be a promising material for enhancing raw biochar's phosphorus removal ability. Thus, this Fe/N co-modification method introduces a practical approach to developing more effective phosphate adsorbents.

5. Limitations and Future Perspectives

In this study, although the Fe/N co-modification method greatly enhanced the adsorption capacity compared to pristine biochar and attapulgite, there is still room for improvement. Other types of biochar, made from various raw materials, varying pyrolysis conditions, and different modification techniques, may achieve higher adsorption capacities than that of Fe/N-BC. Therefore, future research should focus on improving the Fe/N co-modification process, such as adjusting the pyrolysis temperature and the $FeCl_3$-to-urea ratio, to improve adsorption kinetics and capacity and reduce micropore-related mass transfer limits. Also, researchers should gain a more thorough understanding of how iron and nitrogen work together at the molecular level. This understanding can help with the design of more selective and efficient phosphate adsorbents.

Additionally, this study did not investigate the regeneration potential of Fe/N-BC after phosphate saturation. Therefore, in practical applications, more research is needed to study the reusability and applications of the phosphate-saturated adsorbent, such as in the form of slow-release fertilizer. Moreover, testing Fe/N-BC in different types of real water bodies, like polluted rivers or reservoirs, will help confirm whether the material performs well under more complex, real-world conditions. These future efforts are vital in addressing eutrophication, supporting sustainable resource recovery, and promoting the large-scale applications of biochar.

References

Cheng, N., Wang, B., Wu, P., Lee, X., Xing, Y., Chen, M., & Gao, B. (2021). Adsorption of emerging contaminants from water and wastewater by modified biochar: A review. *Environmental Pollution, 273,* 116448. URL: https://doi.org/10.1016/j.envpol.2021.116448

Cui, Q., Xu, J., Wang, W., Tan, L., Cui, Y., Wang, T., Li, G., She, D., & Zheng, J. (2020). Phosphorus recovery by core-shell γ-Al_2O_3/Fe_3O_4 biochar composite from aqueous phosphate solutions. *Science of The Total Environment, 729,* 138892. URL: https://doi.org/10.1016/j.scitotenv.2020.138892

Hou, L., Liang, Q., & Wang, F. (2020). Mechanisms that control the adsorption–desorption behavior of phosphate on magnetite nanoparticles: The role of particle size and surface chemistry characteristics. *RSC Advances,* – 10(4). – P. 2378–2388. URL: https://doi.org/10.1039/C9RA08517C

Huang, R., Lu, X., Li, W., Xiong, J., & Yang, J. (2024). Progress on the adsorption characteristics of nZVI and other iron-modified biochar for phosphate adsorption in water bodies. *Circular Economy,* – 3(4). – 100112 p. URL: https://doi.org/10.1016/j.cec.2024.100112

Li, B., Jing, F., Hu, Z., Liu, Y., Xiao, B., & Guo, D. (2021). Simultaneous recovery of nitrogen and phosphorus from biogas slurry by Fe-modified biochar. *Journal of Saudi Chemical Society,* – 25(4). – 101213 p. URL: https://doi.org/10.1016/j.jscs.2021.101213

Li, S., Ma, X., Ma, Z., Dong, X., Wei, Z., Liu, X., & Zhu, L. (2021). Mg/Al-layered double hydroxide modified biochar for simultaneous removal phosphate and nitrate from aqueous solution. *Environmental Technology & Innovation,* – 23. – P. 101771. URL: https://doi.org/10.1016/j.eti.2021.101771

Li, X., & Shi, J. (2022). Simultaneous adsorption of tetracycline, ammonium and phosphate from wastewater by iron and nitrogen modified biochar: Kinetics, isotherm, thermodynamic and mechanism. *Chemosphere,* – 293. – 133574 p. URL: https://doi.org/10.1016/j.chemosphere.2022.133574

Li, Y., He, X., Hu, H., Zhang, T., Qu, J., & Zhang, Q. (2018). Enhanced phosphate removal from wastewater by using in situ generated fresh trivalent Fe composition through the interaction of Fe(II) on CaCO3. *Journal of Environmental Management*, – 221. – P. 38–44. URL: https://doi.org/10.1016/j.jenvman.2018.05.018

Li, Y., Xu, R., Wang, H., Xu, W., Tian, L., Huang, J., Liang, C., & Zhang, Y. (2022). Recent advances of biochar-based electrochemical sensors and biosensors. *Biosensors,* – 12(6). – 377 p. URL: https://doi.org/10.3390/bios12060377

Li, Z., Liu, X., & Wang, Y. (2020). Modification of sludge-based biochar and its application to phosphorus adsorption from aqueous solution. *Journal of Material Cycles and Waste Management,* – 22(1). – P. 123–132. URL: https://doi.org/10.1007/s10163-019-00921-6

Lin, F., Wang, L., Dai, X., Man, Z., Meng, Y., Chu, D., Yang, Y., Wang, W., Xiao, H., & Wang, K. (2024). Catalytic fixation of hydrogen sulfide over CuO–$CaCO_3$ co-impregnated tea stalk-derived biochar. *Journal of Environmental Chemical Engineering,* – 12(5). – 113320 p. URL: https://doi.org/10.1016/j.jece.2024.113320

Liu, S., Zhao, C., Wang, Z., Ding, H., Deng, H., Yang, G., Li, J., & Zheng, H. (2020). Urea-assisted one-step fabrication of a novel nitrogen-doped carbon fiber aerogel from cotton as metal-free catalyst in peroxymonosulfate activation for efficient degradation of carbamazepine. *Chemical Engineering Journal,* – 386. – 124015 p. URL: https://doi.org/10.1016/j.cej.2020.124015

Luo, D., Wang, L., Nan, H., Cao, Y., Wang, H., Kumar, T. V., & Wang, C. (2023). Phosphorus adsorption by functionalized biochar: A review. *Environmental Chemistry Letters,* – 21(1). – P. 497–524. URL: https://doi.org/10.1007/s10311-022-01519-5

Mei, Y., Xu, J., Zhang, Y., Li, B., Fan, S., & Xu, H. (2021). Effect of Fe-N modification on the properties of biochars and their adsorption behavior on tetracycline removal from aqueous solution. *Bioresource Technology,* – 325. – 124732 p. URL: https://doi.org/10.1016/j.biortech.2021.124732

Pan, F., Wei, H., Huang, Y., Song, J., Gao, M., Zhang, Z., Teng, R., & Jing, S. (2024). Phosphorus adsorption by calcium chloride-modified buckwheat hulls biochar and the potential application as a fertilizer. *Journal of Cleaner Production,* – 444. – 141233 p. URL: https://doi.org/10.1016/j.jclepro.2024.141233

Ping, Q., Zhang, B., Zhang, Z., Lu, K., & Li, Y. (2023). Speciation analysis and formation mechanism of iron-phosphorus compounds during chemical phosphorus removal process. *Chemosphere,* – 310. – 136852 p. URL: https://doi.org/10.1016/j.chemosphere.2022.136852

Qian, L., Zhonghua, Y., Wei, Y., Minghui, Y., Fengpeng, B., Yao, Y., & Yufeng, R. (2023). Tracing the sources and transport of the total phosphorus in the upper Yangtze River. *Ecological Informatics,* – 77. – 102230 p. URL: https://doi.org/10.1016/j.ecoinf.2023.102230

Shin, H., Tiwari, D., & Kim, D.-J. (2020). Phosphate adsorption/desorption kinetics and P bioavailability of Mg-biochar from ground coffee waste. *Journal of Water Process Engineering,* – 37. – 101484 p. URL: https://doi.org/10.1016/j.jwpe.2020.101484

Singh, J., Bhattu, M., Liew, R. K., Verma, M., Brar, S. K., Bechelany, M., & Jadeja, R. (2025). Transforming rice straw waste into biochar for advanced water treatment and soil amendment applications. *Environmental Technology & Innovation,* – 37. – 103932 p. URL: https://doi.org/10.1016/j.eti.2024.103932

United Nations Environment Programme. (2024, January 24). What is phosphorus and why are concerns mounting about its environmental impact? *UNEP*. URL: https://www.unep.org/news-and-stories/story/what-phosphorus-and-why-are-concerns-mounting-about-its-environmental-impact

Wu, B., Wan, J., Zhang, Y., Pan, B., & Lo, I. M. C. (2020). Selective Phosphate Removal from Water and Wastewater using Sorption: Process Fundamentals and Removal Mechanisms. *Environmental Science & Technology*, – 54(1). – P. 50–66. URL: https://doi.org/10.1021/acs.est.9b05569

Xiang, X., Guo, L., Wu, X., Ma, X., & Xia, Y. (2012). Urea formation from carbon dioxide and ammonia at atmospheric pressure. *Environmental Chemistry Letters*, – 10(3). – P. 295–300. URL: https://doi.org/10.1007/s10311-012-0366-2

Yang, J., Zhou, L., Zhao, L., Zhang, H., Yin, J., Wei, G., & Yu, C. (2011). A designed nanoporous material for phosphate removal with high efficiency. *Journal of Materials Chemistry,* – 21(8). – P. 2489–2494. URL: https://doi.org/10.1039/C0JM02718A

Yi, Y., Wang, X., Ma, J., & Ning, P. (2021). Fe(III) modified *Egeria najas*-driven biochar for highly improved reduction and adsorption performance of Cr(VI). *Powder Technology,* – 388. – P. 485–495. URL: https://doi.org/10.1016/j.powtec.2021.04.066

Zhou, X., Liu, Y., Zhou, J., Guo, J., Ren, J., & Zhou, F. (2018). Efficient removal of lead from aqueous solution by urea-functionalized magnetic biochar: Preparation, characterization and mechanism study. *Journal of the Taiwan Institute of Chemical Engineers,* – 91. – P. 457–467. URL: https://doi.org/10.1016/j.jtice.2018.04.018

Zubrowska-Sudol, M., & Walczak, J. (2015). Enhancing combined biological nitrogen and phosphorus removal from wastewater by applying mechanically disintegrated excess sludge. *Water Research,* – 76. – P. 10–18. URL: https://doi.org/10.1016/j.watres.2015.02.041

submitted 10.08.2025;
accepted for publication 24.08.2025;
published 30.09.2025

Contact: ymgao07@gmail.com